IEEE Access
Multidisciplinary | Rapid Review | Open Access Journal

Received July 13, 2019, accepted July 23, 2019, date of publication August 5, 2019, date of current version August 21, 2019.

Digital Object Identifier 10.1109/ACCESS.2019.2932969

Impact of Typhoon on Evaporation Duct in the Northwest Pacific Ocean

YANG SHI[1], QI ZHANG[2], SHUWEN WANG[3], KUNDE YANG[3], YIXIN YANG[3], (Member, IEEE), AND YUANLIANG MA[3]

[1]College of Ocean and Atmospheric Sciences, Ocean University of China, Qingdao 266100, China
[2]School of Marine Sciences, Nanjing University of Information Science and Technology, Nanjing 210044, China
[3]School of Marine Science and Technology, Northwestern Polytechnical University, Xi'an 710072, China

Corresponding author: Kunde Yang (ykdzym@nwpu.edu.cn)

This work was supported in part by the China Postdoctoral Science Foundation under Project 2018M632723, and in part by the State Key Laboratory of Acoustics, Chinese Academy of Sciences under Grant SKLA201804.

ABSTRACT Evaporation duct is a layer above the ocean surface due to the inherent humidity inversion at the air-sea boundary layer. The formation of the duct depends on meteorological factors near the ocean surface and is affected by weather process above the ocean. The presence of this duct can have profound effects on over-water electromagnetic propagation at microwave bands. However, the information on evaporation duct features during the period of typhoon is limited. Here we show the impact of a typhoon on evaporation duct using the typhoon Parpiroon occurred in 2012 as an example. It is very interesting to find that there is an ''evaporation duct eye'' with very low evaporation duct height in the eye of typhoon. The trajectory of the typhoon center is almost consistent with that of the evaporation duct height minimum center during the typhoon Parpiroon. This is also confirmed by 19 more typhoons over northwest Pacific Ocean in 2018. Furthermore, we found that the low wind speed in the typhoon center is the primary cause of this interesting phenomenon. Our results demonstrate the characteristics of evaporation duct distribution during the typhoon process and illustrate the correlation between typhoon trajectory and evaporation duct height minimum center trajectory.

INDEX TERMS Evaporation duct, typhoon Parpiroon, NCEP CFSV2, evaporation duct model, typhoon eye.

I. INTRODUCTION

Evaporation ducts are formed due to the inherent humidity inversion at air-sea boundary. The air in contact with the sea is saturated with water vapor and the water vapor decreases approximately as a logarithmic function of height, creating an evaporation duct structure [1], [2]. Evaporation ducts impact electromagnetic propagation significantly at microwave frequencies greater than 0.5 GHz [3]. The trapping layer of an evaporation duct behaves like a waveguide and can lead to decreased propagation loss at microwave frequencies and an extended radar detection range [4]–[7]. The height at which a radio wave's curvature equals the Earth curvature is defined as the evaporation duct height (EDH) [8], [9]. The EDH is an important parameter for quantifying the near-surface microwave propagation [10], [11]. Evaporation ducts exist extensively over the ocean and the world average EDH is about 13 m [12].

The EDH can be determined by different methods, such as direct measurements [1], inversion methods [2], [13] and numerical models [14]–[18]. In recent years, a number of evaporation duct models, such as the Paulus–Jeske (PJ) model [8], the Musson–Gauthier–Bruth (MGB) model [9], the Liu–Katsaros–Businger (LKB) model [1], the Babin–Young–Carton (BYC) model [14], [15] and the Naval Postgraduate School (NPS) model [16], [17], have been developed to calculate the EDH. Babin tested the PJ, NPS, BYC, MGB and NRL models carefully using ocean buoy data. He found that the NPS model is the optimum model for estimating the modified refractivity profile. However, the NPS model is considered to overestimate the EDH, especially in the stable atmospheric boundary layer. Cheng and Brutseaert [19] and Grachev [20] examined the stability functions of momentum, φ_m, and sensible heat, φ_h,

The associate editor coordinating the review of this manuscript and approving it for publication was Haiyong Zheng.

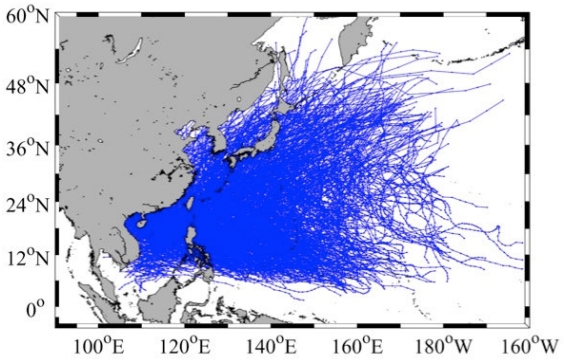

FIGURE 1. Tropical cyclone tracks from 1980 to 2017 in northwest pacific ocean.

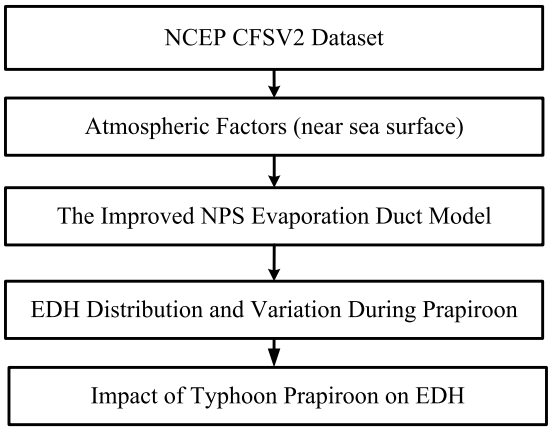

FIGURE 2. Flow diagram of the research.

separately in the stably stratified boundary layer based on a recent boundary layer experiment. Improved stability functions were determined, which may improve the NPS model's performance in stable conditions.

An evaporation duct is formed when the atmospheric index of refractivity sharply decreases with altitude. The index of refractivity is affected by atmospheric processes such as precipitation and tropical cyclones over the ocean. A typhoon is mature tropical cyclone that develops in the northwestern part of the Pacific Ocean from 100°E to 180°E and 0° to 60°N, which is referred to as the northwest Pacific basin. The majority of storms form between June and November, while tropical cyclone formation is at minimum between December and May. On average, the northwest Pacific has the greatest frequency and highest intensity of tropical cyclones globally as it is shown in Fig.1 [21]. During the typhoon process, atmospheric parameters near the sea surface may change quickly and have an important impact on the EDH [22], [23]. However, the impacts of typhoon on evaporation duct are seldom reported. As a result, it is of great importance to investigate the impact of typhoons on evaporation ducts in the northwest Pacific. Meanwhile, recent improvements in both evaporation duct models and the temporal-spatial resolution of the National Centers for Environmental Prediction (NCEP) Climate Forecast System Version 2 (CFSV2) dataset [24] make it possible to study the impact of typhoons on the EDH. This data set has been widely used in the evaporation duct climatology analysis and proven to be in a good reliability to estimate the actual EDH [25], [26].

This study focuses on the typhoon impact on the evaporation duct. An improved evaporation duct model with better performance in stable conditions is introduced. Then, the improved model and the NCEP CFSV2 dataset are used to compute the EDH distribution and variation during typhoon period. Finally, the impacts of typhoon on the evaporation duct is analyzed.

II. MATERIALS AND METHODS

A research flowchart of this study is shown in Fig. 2. Firstly, the NCEP CFSV2 dataset during typhoon Prapiroon was obtained from the Computational and Information Systems Laboratory (CISL) Research Data Achieve managed by NCAR's data support section. Secondly, the atmospheric parameters near the sea surface, such as air temperature, relative humidity, sea surface temperature, wind speed and sea surface pressure, were obtained from the NCEP CFSV2 dataset. Thirdly, the above atmospheric parameters were input to the improved NPS evaporation duct model to calculate the EDH in the northwest Pacific during typhoon period. Fourthly, EDH distribution and variation during typhoon period were analyzed. Finally, the physical mechanism of the impact of typhoon on the evaporation duct are discussed. In this section, the improved NPS evaporation duct model, the NCEP CFSV2 dataset and information about typhoon Prapiroon are separately introduced.

A. IMPROVED NPS MODEL

The current NPS model [16], [17] depends on the empirically determined Moni–Obukhov similarity theory dimensionless profile function in stable conditions (air–sea temperature difference (ASTD) >0°C). The current NPS model was considered to overestimate EDH, especially in strongly stable conditions. The improved NPS model is much less sensitive to input parameters and has a much wider region of applicability over which the EDH can be defined in stable conditions when using the two improved stability functions determined by Cheng and Brutseaert [19] and Grachev *et al.* [20].

Fig. 3 shows the modified refractivity profile calculated using different φ functions which indicates the stability of atmosphere. In Fig. 3, M is short for modified refractivity and M unit is the unit of the modified refractivity. Figs. 4–6 show the EDH sensitivity analysis in stable conditions using three stability functions (the current NPS, Cheng (2005) and Grachev (2007)). The atmospheric parameters near the sea surface are shown in Table 1 and these values are chosen to represent the typical atmospheric conditions in the northwest Pacific Ocean.

In Fig.3, the three examples show the effectiveness of three different NPS models in calculating the EDH using different stability functions. The green line shows the modified

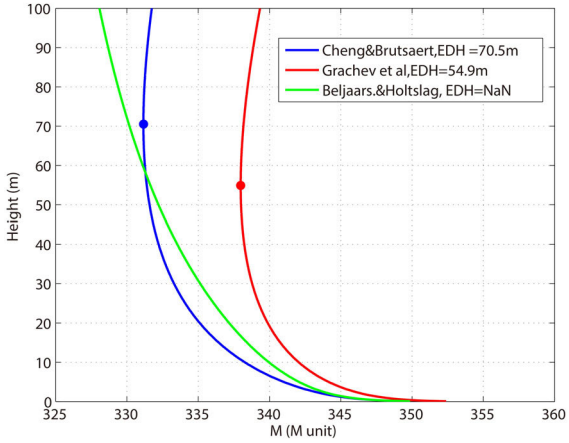

FIGURE 3. Modified refractivity profiles calculated using different φ functions.

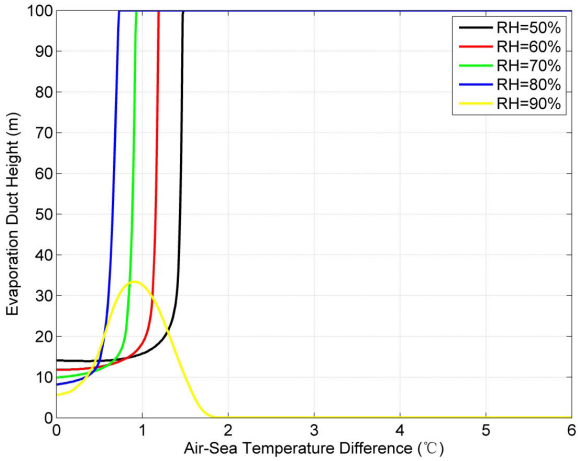

FIGURE 4. EDH sensitivity analysis with the current NPS model.

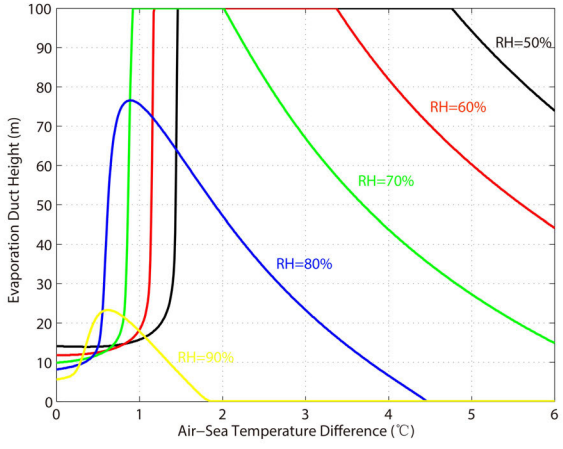

FIGURE 5. EDH sensitivity analysis with cheng and brutsaert (2005)'s stability function.

refractivity profiles calculated by the current NPS model based on Beljaar and Holtslag's stability function. The current NPS model cannot define the EDH in this stable condition (ASTD = 2°C) because under such condition Beljaar and Holtslag's stability function may be invalid. The blue line

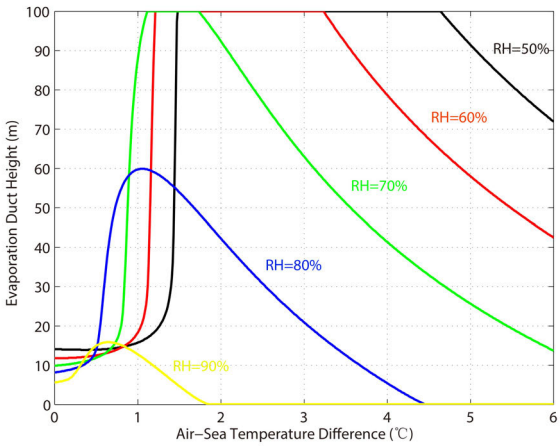

FIGURE 6. EDH sensitivity analysis with grachev(2007)'s stability function.

TABLE 1. Atmospheric parameters used in Figs. 3–6.

Variable Name	Fig.3	Fig.4-Fig.6
Air Temperature (□)	20	25
Air-Sea Temperature Difference (□)	2	0-6
Relative Humidity (%)	72	50%-90%
Wind Speed (m/s)	5.3	3
Sea Surface Pressure(hPa)	1022.2	1000

shows the result calculated based on Cheng and Brutsaert's stability function, which defines the EDH as 70.5 m. The red line shows the result based on Grachev's stability function, which defines the EDH as 54.9 m.

Figs. 4–6 show the EDH sensitivity analysis results using the current NPS model, the Cheng stability function and the Grachev stability function, respectively. The ASTD varies from 0°C to 6°C and the relative humidity varies from 50% to 90%. As shown in Fig. 4, the current NPS model cannot define the EDH when the ASTD is greater than 2°C in low relative humidity conditions. The improved NPS model with the two new stability functions has a much wider region of applicability in stable conditions, especially with the Grachev stability function (Fig. 6). The three modified refractivity profiles to the Advanced Propagation Model to determine the propagation conditions and validate the improved NPS models. It was concluded that the improved NPS model with the Grachev stability function produces the best agreement with propagation measurements. Therefore, the improved NPS model with the Grachev stability function was chosen to compute the EDH in this study.

B. NCEP CFSV2 DATASET

The NCEP reanalysis data provide an effective method to investigate the impact of typhoons on evaporation ducts. The NCEP and National Center for Atmospheric Research (NCAR) are cooperating in the reanalysis project to produce a record of global analyses of atmospheric fields in

TABLE 2. Primary factors from NCEP CFSR and calculated factors.

PRIMARY FACTORS	Reanalysis height(m)	Units	Abbreviation
Air Temperature	2m	□	TA
Skin Temperature	Surface	□	
Specific Humidity	2m	g/kg	SH
u component of wind	10m	m/s	
v component of wind	10m	m/s	
Sea Level Pressure	Surface	hPa	SLP
CALCULATED FACTOR			
Wind Speed	10m	m/s	WS
Air-Sea Temperature Difference	2m	□	ASTD
Relative Humidity	2m	%	RH
Evaporation Duct Height	NA	m	EDH

support of the research and climate monitoring communities. These efforts involve the recovery of observation data from land, surface, ships, radiosonde, aircraft and satellites, and quality control and assimilation of these data using a data assimilation system that remains unchanged over the reanalysis period. The NCEP CFSR [24] product was completed for the 31-year period of 1979 to 2009 in January 2010. The CFSR was designed and executed as a global, high-resolution, coupled atmosphere–ocean–land surface–sea ice system to provide the best estimate of the state of these coupled domains over this period. One-hour reanalysis data are available from 1979 to the present day and global atmospheric fields are provided for a variety of atmospheric parameters. The spatial coverage is 1152 × 576 grid points from 0°E to 359.687°E and 89.761°N to 89.761°S, which provides data with a high horizontal resolution (0.313°× 0.312°). From 1 January 2011, CFSR has been extended by NCEP's Climate Forecast System Version 2 (CFSV2) operational model. The data produced by CFSV2 can be considered as a seamless extension to CFSR, except that the resolution of surface and flux fields was increased from 0.3° in CFSR to approximately 0.2° in CFSV2. The improved spatial resolution is useful for analyzing the impact of typhoons on evaporation ducts.

As typhoon Prapiroon occurred in October 2012, the NCEP CFSV2 dataset in October 2012 was obtained from the CISL Research Data Achieve. Compared with the previous NCEP CFSR reanalysis data, the spatial resolution of the surface and flux fields was increased to about 0.2° and the time resolution remained the same (1 hour). Table 2 shows the atmospheric parameters obtained from NCEP CFSV2 and those calculated in this study.

C. TYPHOON DATA

The Typhoon data are obtained from China Meteorological Administration (CMA). Fig.7 shows the typhoon tracks used in our study, in which the blue ones are the typhoons in 2018 and the red one is the Typhoon Prapiroon. Typhoon Prapiroon is chosen as an case study to because it has no

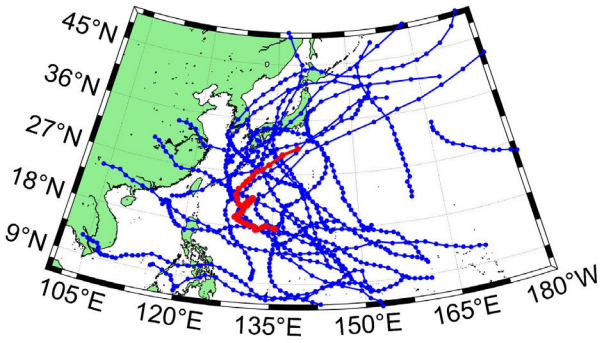

FIGURE 7. Typhoon tracks used in the study. Typhoons in 2018 are depicted in blue, and Typhoon Prapiroon is in red.

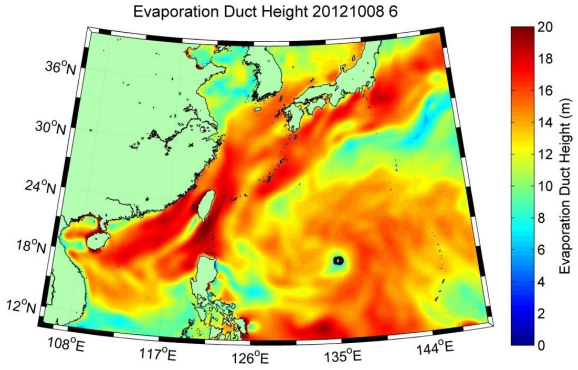

FIGURE 8. EDH distribution in northwest pacific ocean at 06:00 on 8 October 2012.

interaction with land. Thus, the formation of evaporation duct is only affected by the atmosphere and ocean.

III. RESULTS

The hourly EDH distribution in the northwest Pacific Ocean during the typhoons was calculated. Fig. 8 shows the EDH distribution in the northwest Pacific Ocean at 06:00 (UTC) on 8 October 2012. At that time, typhoon Prapiroon was located at 18.1°N, 135°E as indicated by the square in Fig. 8. Its maximum sustained winds were near 24.7m/s and it was moving westward at 2.8m/s. Typhoon Prapiroon had an important effect on the EDH distribution in the northwest Pacific Ocean. It is very interesting to find that there is an ''evaporation duct eye'' with very low EDH in the eye of typhoon. The circle in Fig. 8 indicates the position of the lowest EDH and it is almost in the same position as the eye of typhoon. Fig. 9 shows the EDH distribution during typhoon Prapiroon at selected hours. The same phenomenon can be found, that is, the EDH is very low near the eye of typhoon. In this study, the position with the minimum EDH is defined as EDH minimum center. The EDH minimum center is calculated during typhoon Prapiroon.

Fig. 10 shows the track comparison of typhoon Prapiroon and the EDH minimum center. The red circles represent the typhoon Prapiroon center and the green circles represent the EDH minimum center. It is interesting to find that these two tracks are almost consistent with each other during the

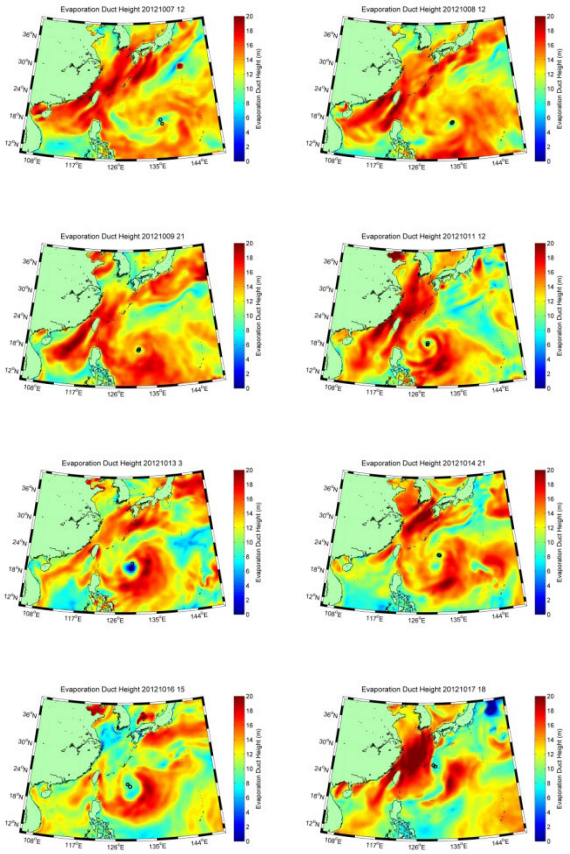

FIGURE 9. EDH distribution in northwest pacific ocean at selected hours during typhoon Prapiroon.

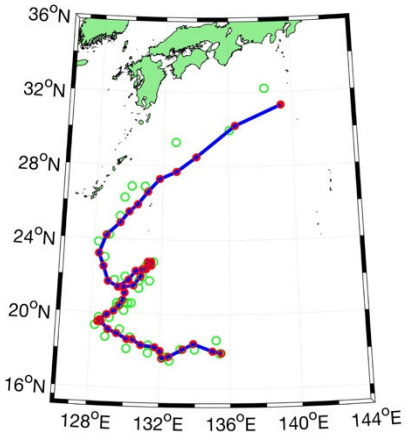

FIGURE 10. Track of typhoon prapiroon center and EDH minimum center (red circles: Typhoon center; green circles: EDH minimum center).

whole typhoon process. To illustrate this phenomenon more clear, we created the scatterplots (Fig.11) to compare the latitude and longitude of the EDH minimum center with related typhoon center, respectively. It also can be concluded that the typhoon center was almost at the same position as the EDH minimum center during the entire typhoon process. Further, we also conduct the same analysis to the typhoons that occurring in 2018 and the results shows the same outcome (Fig.12).

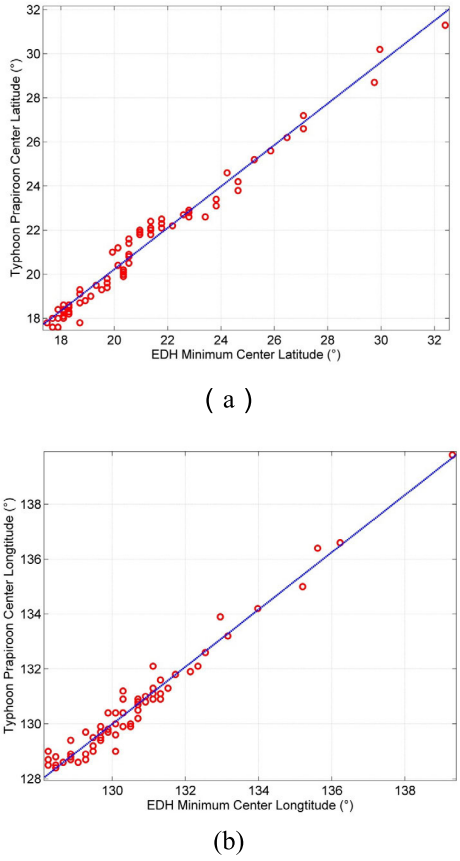

FIGURE 11. Comparison of EDH minimum center and typhoon prapiroon center. (a) Latitude. (b) Longitude.

IV. DISCUSSION

In this section, the physical principles underlying the consistency between the typhoon center and EDH minimum center are discussed using typhoon Prapiroon. The time point of 18:00 (UTC) on 8 October (Fig. 13) is chosen as an example, and similar results can be obtained at other times during the typhoon period. At this time, typhoon Prapiroon was located at 18°N, 133.2°E. Its maximum sustained winds were near 28m/s and it was moving westward at 2.2m/s.

Fig. 14 shows some of the atmospheric parameters during typhoon Prapiroon: sea surface pressure, air temperature, relative humidity and wind speed. In the typhoon center, the sea surface pressure was low, about 980 hPa, and the wind speed was almost about 0 m s^{-1}. The wind speed increased to about 16 m s^{-1} far from the typhoon center. The sea surface pressure also increased far from the typhoon center. The relative humidity was relatively high in the southeast of the typhoon center, approximately 90%, and the air temperature was about 28°C in the area around the typhoon center.

In particular, the latitudinal and longitudinal features of the EDH and atmospheric parameters were investigated to determine the physical principles underlying the consistency between the typhoon center and the EDH minimum center. Figs. 15 and 16 show the features of the EDH and atmospheric parameters along 18.09°N and 133.16°E, respectively.

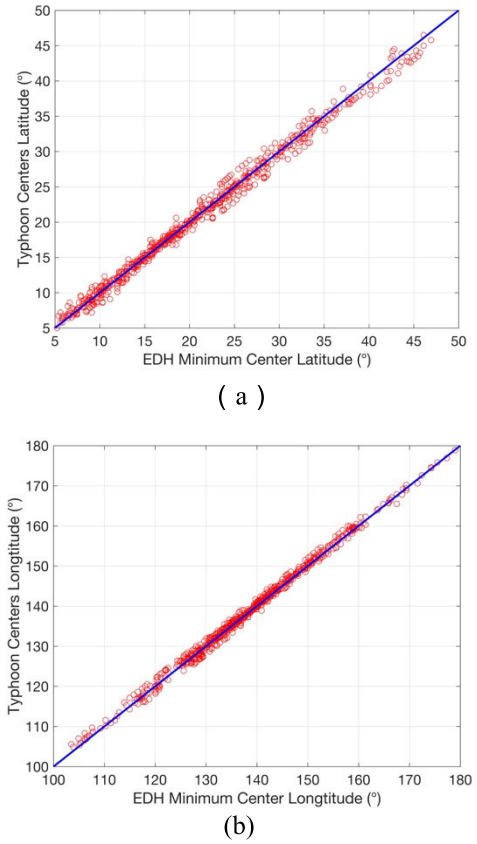

FIGURE 12. Comparison of EDH minimum centers and the centers of typhoon in 2018. (a) Latitude. (b) Longitude.

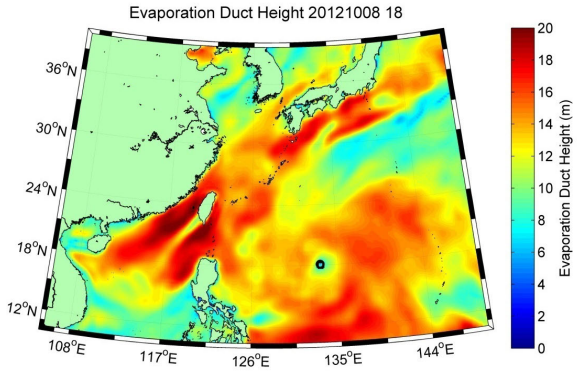

FIGURE 13. EDH distribution on 18:00 (UTC) on 8 October 2012.

Fig. 15 shows that the EDH remained at about 14 m from 127°E to 131°E and began to decrease at 132°E. The EDH reached a minimum (about 6 m) at the typhoon center and then began to increase. It reached about 15 m at 136°E and remained almost the same from 137°E to 139°E. Similar features can be obtained with wind speed and sea surface pressure. It should be noted that the wind speed decreased to 0 m s^{-1} at the typhoon center. The relative humidity slightly decreased near the typhoon center and remained above 80% in most cases. The ASTD remained below 0°C and is in the unstable condition along 18.09°N. Similar results can be obtained along 133.16°E, as shown in Fig. 16.

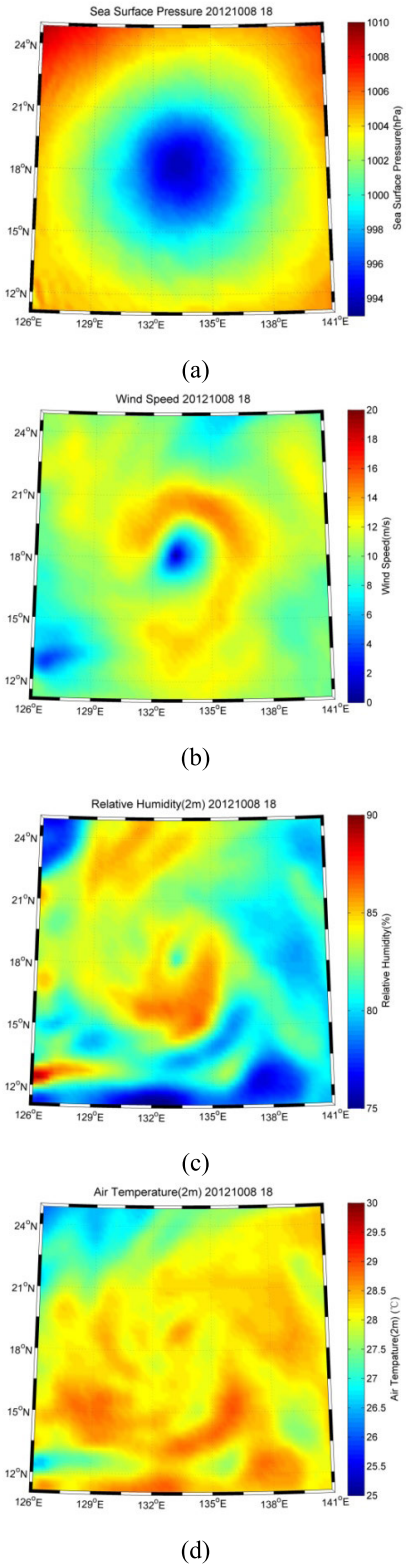

FIGURE 14. Atmospheric parameters during typhoon prapiroon at 18:00 (UTC) on 8 October. (a) Sea surface pressure. (b) Wind speed (10 m). (c) Relative humidity (2 m). (d) Air temperature (2 m).

Fig. 17 shows the relationship between the EDH and atmospheric parameters along 133.16°E. It can be seen that

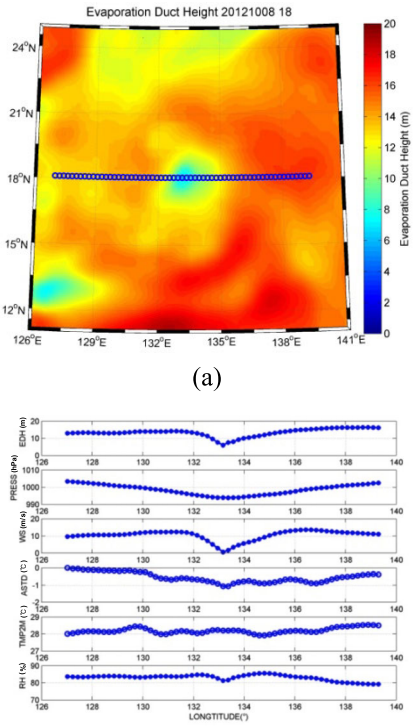

FIGURE 15. EDH and atmospheric factors features along 18.09°N. (a) EDH. (b) Atmospheric factors.

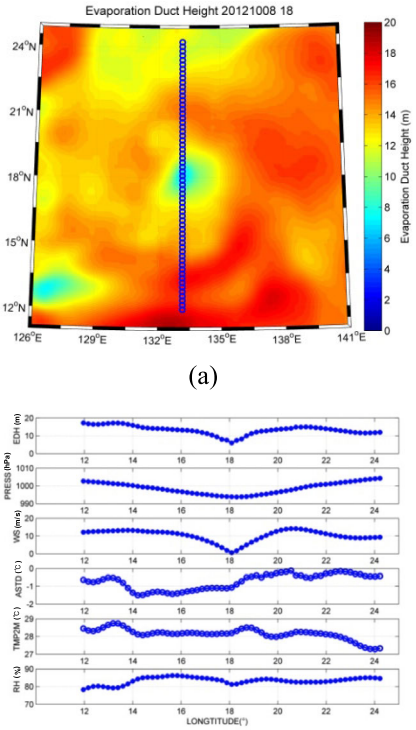

FIGURE 16. EDH and atmospheric factors features along 133.16°E. (a) EDH. (b) Atmospheric factors.

the wind speeds have an almost linear relationship with the EDH when the EDH is less than 15 m. However, the other

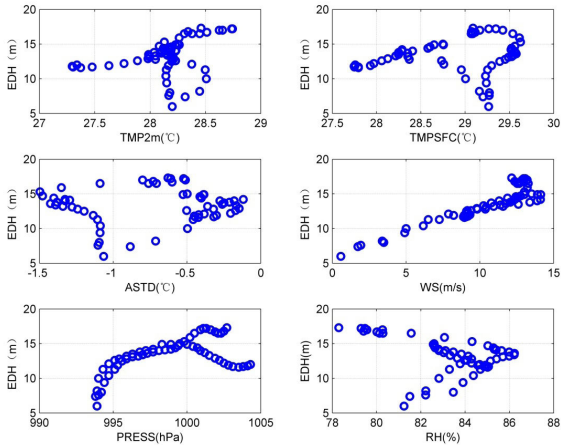

FIGURE 17. Relationship between EDH and atmospheric parameters along 133.16°E.

atmospheric parameters do not have an obvious relationship with the EDH. As a result, the wind speed may be the primary cause of the low EDH in the typhoon center.

As stated in section 2.1, the NPS evaporation duct model can be used to study the EDH sensitivity with the atmospheric parameters near the ocean surface. The model is used to study the primary cause of the low EDH in the typhoon center by analyzing the EDH sensitivity under atmospheric conditions during typhoon Prapiroon.

Fig. 18(a) shows the impact of the wind speed on the EDH. In the calculation, the relative humidity was set as 85% and the air temperature (2 m) was set as 28°C, which are the average values near the typhoon Prapiroon center. It is shown that the EDH decreases quickly with decreasing wind speed when the EDH is less than 15 m, which is consistent with the analysis in Fig. 17. Under these atmospheric conditions, the influence of the ASTD is small. Fig. 18(b)–(d) shows the impact of the ASTD, sea surface pressure and relative humidity on the EDH under different wind speeds. It can be seen that the sea surface pressure has the least impact on the EDH (Fig. 18(c)). The EDH slightly changes with the increasing ASTD and relative humidity. When the EDH is less than 15 m, these two factors' impacts are less than the wind speed's impact (Fig. 18(b), (d)). To summarize, low wind speed is the primary physical cause of the low EDH in the typhoon Prapiroon center.

V. CONCLUSION

The impact of typhoon on the evaporation duct was studied in this paper. It is very interesting to find that there is an ''evaporation duct eye'' with very low EDH in the eye of typhoon. The trajectory of the typhoon center is almost the same as that of the EDH minimum center. The physical principle of this interesting phenomenon was illustrated based on the evaporation duct model and it is found that the low wind speed in the typhoon center is the primary cause. The impact of evaporation duct on electromagnetic propagation during the typhoon process needs to be investigated in the future.

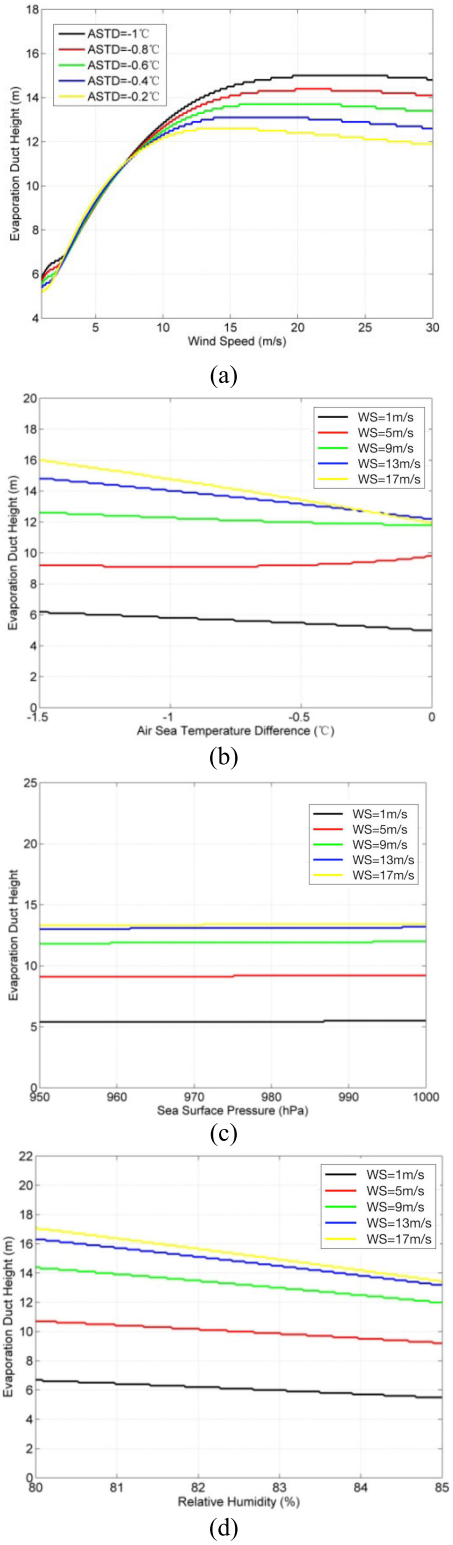

FIGURE 18. EDH sensitivity analysis during typhoon prapiroon. (a) Wind Speed. (b) Air sea temperature difference. (c) Sea surface pressure. (d) Relative humidity.

Meanwhile, owing to the limitation of the spatial resolution of NCEP CFSV2, there may be some error in the estimation of the EDH minimum center. The data from ocean atmosphere buoys can be used to improve the accuracy of estimation of the EDH minimum center. The relevant experiment validation during the typhoon process should be conducted in the future.

ACKNOWLEDGMENT

The authors also would like to thank the National Center for Atmospheric Research and China Meteorological Administration for providing the reanalysis data sets and typhoon data used in this paper, respectively. The reanalysis data could be obtained through NCAR public website https:// rda.ucar.edu/ and the typhoon data could be obtained from the website http://tcdata.typhoon.org.cn/index.html.

REFERENCES

[1] W. T. Liu, K. B. Katsaros, and J. A. Businger, "Bulk parameterization of air-sea exchanges of heat and water vapor including the molecular constraints at the interface," *J. Atmos. Sci.*, vol. 36, pp. 1722–1735, Apr. 1979.
[2] C. Yardim, "Statistical estimation and tracking of refractivity from radar clutter," Ph.D. dissertation, Univ. California, San Diego, San Diego, CA, USA, 2007.
[3] K. L. Twigg, "A smart climatology of evaporation duct height and surface radar propagation in the Indian Ocean," M.S. thesis, Naval Postgraduate School, Monterey, CA, USA, 2007.
[4] K. D. Anderson, "Radar detection of low-altitude targets in a maritime environment," *IEEE Trans. Antennas Propag.*, vol. 43, no. 6, pp. 609–613, Jun. 1995.
[5] G. S. Woods, A. Ruxton, C. Huddlestone-Holmes, and G. Gigan, "High-capacity, long-range, over ocean microwave link using the evaporation duct," *IEEE J. Ocean. Eng.*, vol. 34, no. 3, pp. 323–330, Jul. 2009.
[6] J. Wang, H. Zhou, Y. Li, Q. Sun, Y. Wu, S. Jin, T. Q. S. Quek, and C. Xu, "Wireless channel models for maritime communications," *IEEE Access*, vol. 6, pp. 68070–68088, 2018.
[7] K. S. Zaidi, V. Jeoti, M. Drieberg, A. Awang, and A. Iqbal, "Fading characteristics in evaporation duct: Fade margin for a wireless link in the South China Sea," *IEEE Access*, vol. 6, pp. 11038–11045, 2018.
[8] R. A. Paulus, "Practical application of an evaporation duct model," *Radio Sci.*, vol. 20, no. 4, pp. 887–896, Jul./Aug. 1985.
[9] L. Musson-Genon, S. Gauthier, and E. Bruth, "A simple method to determine evaporation duct height in the sea surface boundary layer," *Radio Sci.*, vol. 27, no. 5, pp. 635–644, Sep./Oct. 1992.
[10] S. Yang, K.-D. Yang, Y.-X. Yang, and Y.-L. Ma, "Experimental verification of effect of horizontal inhomogeneity of evaporation duct on electromagnetic wave propagation," *Chin. Phys. B*, vol. 24, no. 5, 2015, Art. no. 044102.
[11] S. Yang, Y. Kun-De, Y. Yi-Xin, and M. Yuan-Liang, "Influence of obstacle on electromagnetic wave propagation in evaporation duct with experiment verification," *Chin. Phys. B.*, vol. 24, no. 5, 2015, Art. no. 054101.
[12] K. Yang, Q. Zhang, Y. Shi, Z. He, B. Lei, and Y. Han, "On analyzing space-time distribution of evaporation duct height over the global ocean," *Acta Oceanol. Sin.*, vol. 35, no. 7, pp. 20–29, 2016.
[13] A. Karimian, C. Yardim, P. Gerstoft, W. S. Hodgkiss, and A. E. Barrios, "Multiple grazing angle sea clutter modeling," *IEEE Trans. Antennas Propag.*, vol. 60, no. 9, pp. 4408–4417, Sep. 2012.
[14] S. M. Babin, "A new model of the oceanic evaporation duct and its comparison with current models," Ph.D. dissertation, Univ. Maryland, College Park, MD, USA, 1996.
[15] S. M. Babin, G. S. Young, and J. A. Carton, "A new model of the oceanic evaporation duct," *J. Appl. Meteorol.*, vol. 36, no. 3, pp. 193–204, Mar. 1997.
[16] P. A. Frederickson, K. L. Davidson, and A. K. Goroch, "Operational bulk evaporation duct model for MORIAH version 1.2," Nav. Postgraduate School, Monterey, CA, USA, Tech. Rep., 2000.
[17] P. A. Frederickson, K. L. Davidson, and A. Newton, "An operational bulk evaporation duct model," in *Proc. Battlespace ACIMOC*, Monterey, CA, USA, 2003, p. 1.
[18] Q. Zhang, K. Yang, and Q. Yang, "Statistical analysis of the quantified relationship between evaporation duct and oceanic evaporation for unstable conditions," *J. Atmos. Ocean. Technol.*, vol. 34, no. 11, pp. 2489–2497, Nov. 2017.

[19] Y. Cheng and W. Brutseaert, "Flux-profile relationships for wind speed and temperature in the stable atmospheric boundary layer," *Boundary-Layer Meteorol.*, vol. 114, no. 3, pp. 519–538, 2005.
[20] A. A. Grachev, E. L. Andreas, C. W. Fairall, P. S. Guest, and P. O. G. Persson, "SHEBA flux–profile relationships in the stable atmospheric boundary layer," *Bounday-Lay Meteorol.*, vol. 124, no. 3, pp. 315–333, 2017.
[21] M. Ying, W. Zhang, H. Yu, X. Lu, J. Feng, Y. Fan, Y. Zhu, and D. Chen, "An overview of the China Meteorological Administration tropical cyclone database," *J. Atmos. Ocean. Technol.*, vol. 31, no. 2, pp. 287–301, 2014.
[22] J. Ning, Q. Xu, H. Zhang, T. Wan, and K. Fan, "Impact of cyclonic ocean eddies on upper ocean thermodynamic response to typhoon Soudelor," *Remote Sens.*, vol. 11, no. 8, p. 938, 2019.
[23] K. Xiang, X. Yang, M. Zhang, Z. Li, and F. Kong, "Objective estimation of tropical cyclone intensity from active and passive microwave remote sensing observations in the Northwestern Pacific Ocean," *Remote Sens.*, vol. 11, no. 6, p. 627, 2019.
[24] S. Saha, S. Moorthi, H. L. Pan, X. Wu, J. Wang, S. Nadiga, P. Tripp, R. Kistler, J. Woollen, D. Behringer, and H. Liu, "The NCEP climate forecast system reanalysis," *Bull. Amer. Meteor. Soc.*, vol. 91, no. 8, pp. 1015–1057, Aug. 2010.
[25] P. A. Frederickson, J. T. Murphree, K. L. Twigg, and A. Barrios, "A modern global evaporation duct climatology," in *Proc. IEEE Int. Conf. Radar*, Adelaide, SA, Australia, Sep. 2008, pp. 292–296.
[26] K. Yang, Q. Zhang, and Y. Shi, "Interannual variability of the evaporation duct over the South China Sea and its relations with regional evaporation," *J. Geophys. Res. Oceans.*, vol. 122, no. 8, pp. 6698–6713, 2017.

YANG SHI received the B.S. and M.S. degrees in electronic engineering and the Ph.D. degree in underwater acoustics engineering from Northwestern Polytechnical University, Xi'an, China, in 2009, 2012, and 2017, respectively.

Since September 2017, he has been holding a Postdoctoral position at the College of Oceanic and Atmospheric Science, Ocean University of China, Qingdao, China. His research interests include oceanic microwave propagation, oceanic atmosphere waveguide, and ocean acoustics.

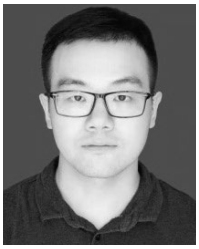

QI ZHANG received the B.S. degree in electronic engineering, the M.S. degree in electromagnetic fields and microwave technology, the Ph.D. degree in underwater acoustics engineering from Northwestern Polytechnical University, in 2010, 2013, and 2018, respectively.

Since July 2018, he has been a Lecturer with the School of Marines, Nanjing University of Information Science and Technology. His research interests include oceanic atmosphere waveguides, oceanic microwave propagation, and ocean acoustics.

SHUWEN WANG received the B.S. degree in underwater acoustic engineering from Northwestern Polytechnical University (NPU), Xi'an, China, in 2018, where he is currently pursuing the Ph.D. degree.

His research interests include oceanic atmosphere waveguides, oceanic microwave propagation, and ocean acoustics.

KUNDE YANG received the B.S., M.S., and Ph.D. degrees in underwater acoustic engineering from Northwestern Polytechnical University (NPU), Xi'an, China, in 1996, 1999, and 2003, respectively.

He was a Visiting Scholar with the School of Earth and Ocean Sciences, University of Victoria, Victoria, BC, Canada, from 2006 to 2007. He has been with the School of Marine Science and Technology, NPU, since 2003, where he is currently a Full Professor and the Director of the Department of Acoustic and Information Engineering. His research interests include ocean acoustic modeling, signal processing, and microwave propagation.

YIXIN YANG (M'03) received the B.S. degree in applied electronic engineering and the M.S. and Ph.D. degrees in underwater acoustic engineering from Northwestern Polytechnical University (NPU), Xi'an, China, in 1997, 1999, and 2002, respectively.

From June 2002 to June 2004, he was a Research Fellow of the School of Electrical and Electronic Engineering, Nanyang Technological University, Singapore, Singapore. Since July 2004, he has been with the School of Marine Science and Technology, NPU, where he is currently a Professor. His current research interests include acoustic array signal processing, spectral estimation, and their applications.

YUANLIANG MA received the bachelor's degree in underwater acoustics through a joint educational program from Northwestern Polytechnical University (NPU), Xi'an, China, and the bachelor's degree from the former Harbin Institute of Military Engineering, Harbin, China, in 1961.

Since 1961, he has been involved in underwater acoustics and signal processing. From 1981 to 1983, he was a Visiting Scholar with the Department of Electronic and Electrical Engineering, Loughborough University, Loughborough, U.K. His current research interests include sensor array signal processing, ocean acoustics, microwave propagation, and signal processing systems. In 1980, he became an Associate Professor with NPU, where he has been a Full Professor, since 1985. His publications include three books, i.e., *Underwater Acoustic Transducers*, *Sensor Array Beam-Pattern Optimization: Theory With applications*, and *Adaptive Active Noise Control*, in addition to over 300 journal and conference papers.

Prof. Ma was elected as a member of the Chinese Academy of Engineering. He is also a Fellow of the Acoustical Society of China and a member of the Acoustical Society of America. He is currently the Chair of the Academic Committee. He was the Vice-President of the Acoustical Society of China and the Chair of its Underwater Acoustics Chapter from 1998 to 2006. He is an Associate Editor of Chinese *Science Bulletin*.